International Journal of Multimedia and Ubiquitous Engineering
Vol. 10, No. 1 (2015), pp. 209-218
http://dx.doi.org/10.14257/ijmue.2015.10.1.20

# Needle Deflection during Insertion into Soft Tissue Based on Virtual Spring Model

Haiyan Du*, Yongde Zhang, Jingang Jiang and Yanjiang Zhao

*Intelligent Machine Institute, Harbin University of Science and Technology, China*
*duhaiyan@hrbust.edu.cn*

***Abstract***

*Needle insertion is the most common procedure of minimally invasive interventions. During insertion into a soft tissue, the needle with bevel tip can deflect due to the asymmetric forces acting on the tip of the needle. In this paper, a mechanics-based model is developed to predict the needle deflection. In the model, the needle is considered as a cantilever beam supported by a series of nonlinear springs each of which has stiffness different from each other. The value of stiffness can be calculated by cutting force acting on the needle tip. Based on the model and the analysis of cutting force and friction force, Rayleigh-Ritz method is used to estimate the amount of needle deflection. Experiment shows that the simulation model can accurately predict the deflection of the bevel-tipped needle.*

***Keywords:*** *Needle deflection, Soft tissue, Cantilever beam model, Rayleigh-Ritz method, Nonlinear spring*

## 1. Introduction

Percutaneous needle insertion is one of the most common minimally invasive surgeries which can be used for biopsy, brachytherapy and local drug delivery. However, accurate positioning of the needle is critical. Currently, the bevel-tipped needle is mainly used in clinic, but it is known that a beveled tip is more susceptible to the tissue density. During insertion the needle deflects towards the direction of the bevel due to the asymmetric forces acting on the tip of the needle [1], which directly affect position accuracy of needle insertion. Therefore, it is very important to establish the needle-tissue interaction model to predict the deflection of needle with beveled tip.

Many efforts have been made to study the needle deflection during needle insertion. In [2-4], the needle was modeled based on beam theory to predict the amount of needle deflection. Abolhassan *et al*. [5] proposed that the needle deflection can be considered as a cantilever beam with a spring support. The stiffness of the support is related to the mechanical properties of soft tissue. In 2007, they proposed to estimates the amount of needle deflection using Euler-Bernoulli beam equations in their "model-based" method [6]. But with their method, in order to compensate the deflection, the needle has to be rotated through 180° when the amount of estimated deflection goes beyond a pre-defined threshold. Roesthuis *et al*. [7] considered needle as a cantilever beam supported by springs which have needle tissue interaction stiffness evaluated by comparing results from experiments and simulation. But the interaction stiffness was assumed to be constant at each location along the needle shaft. In [8], Roesthuis *et al*. presented a mechanics-based model based on Rayleigh-Ritz method. Based on the work by Roesthuis, in [9], an online evaluation method for load distribution is further proposed to determine the distributed load when the needle is inserted into non-homogenous tissue. H. Sadjadi *et al*. [10] present a needle deflection estimation method using fusion of two electromagnetic trackers.

ISSN: 1975-0080 IJMUE

In this paper，a mechanics-based model is developed to predict the amount of a bevel-tipped needle deflection during insertion into soft tissue. The model is built upon the work by the authors in [7]. But in our work, we use a series of nonlinear springs instead of linear springs to model needle-tissue interaction. Each spring has its own stiffness which is different from others throughout the tissue. These developments are more consistent with the nonlinearity and imhomogeneity of soft tissue.

## 2. Needle-tissue Interaction Forces

When a needle is inserted into a soft tissue, forces will be caused on the needle due to its interaction with the surrounding tissue. As shown in Figure 1, the interaction forces during insertion into a soft tissue are decomposed of a friction force along the needle shaft ( $F_f$ ), a cutting force acting normal to the needle's bevel tip ( $F_c$ ) and a friction force along the edge of needle bevel ( $F_t$ ).Due to the smaller size of the needle tip relative to the length of the needle shaft, we may ignore the friction force along the needle bevel. The cutting force is considered to be a result from cutting of the tissue at the needle tip [7], [11]. Furthermore, due to the cutting force and asymmetry of the bevel tip, the needle has to bend, resulting that it is subjected to a resistance force from the tissue ( $F_s$ ).

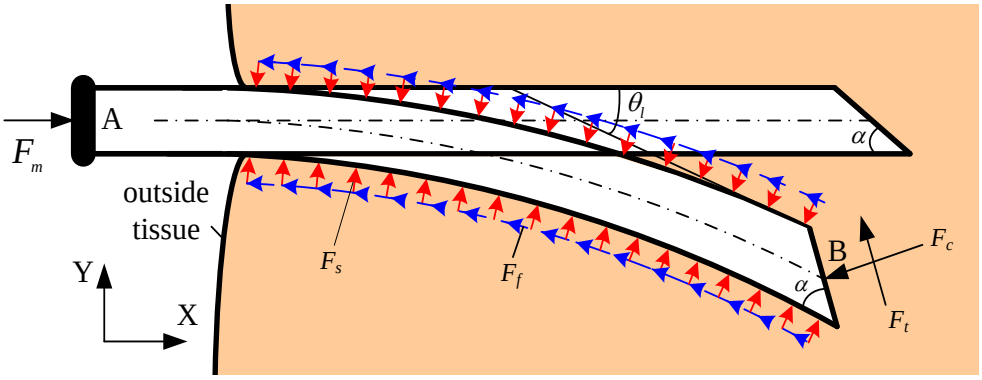


**Figure 1. Interaction Forces During Needle Insertion into a Soft Tissue**

### 2.1. Cutting Force on the Needle Tip

As the needle tip cuts through a soft tissue, it moves the soft tissue away and takes the place of tissue. The deformation of tissue as the needle tip moves forward caused a triangular distributed load ( $\delta(\eta)$ ) along the edge of needle tip [12], shown in Figure 2. In Figure 2, $d$ and $\alpha$ are the diameter of the needle and the bevel angle respectively, we define the variable $b$ as:

$$b = d / \sin\alpha \tag{1}$$

The triangular load $\delta(\eta)$ meets the following formula:

$$\delta(\eta) = K_t \eta \tan\alpha \tag{2}$$

where $K_t$ is the interaction stiffness of the needle-tissue per unit length

The load $\delta(\eta)$ along the bevel of needle tip can be simplified to a resultant forces named as cutting force ( $F_c$ ) on the *b*/3 of the edge of bevel tip, which is:

$$F_c = \int_0^b \delta(\eta) d\eta = \frac{K_t b^2}{2} \tan\alpha \tag{3}$$

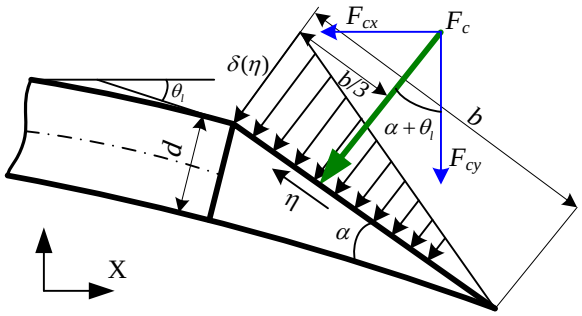


**Figure 2. Cutting Force Acting on the Needle Tip**

According to (1) and (3), $F_c$ can be derived as:

$$F_c = \frac{K_t (d / \sin\alpha)^2}{2} \tan\alpha = \frac{K_t d^2}{\sin 2\alpha} \tag{4}$$

The cutting force is composed of components acting in the X-direction and Y-direction. Using the needle slope ($\theta(x)$), the components ($F_{cx}$ and $F_{cy}$) of the cutting force ($F_c$) can be calculated by

$$F_{cx} = F_c \sin(\alpha + \theta_l) = \frac{K_t d^2}{\sin 2\alpha} \sin(\alpha + \theta_l) \tag{5}$$

$$F_{cy} = F_c \cos(\alpha + \theta_l) = \frac{K_t d^2}{\sin 2\alpha} \cos(\alpha + \theta_l) \tag{6}$$

where $\theta_l$ is the slope of needle tip, and $\theta_l = \theta(x)|_{x=l}$.

### 2.2. Friction Force along Needle Shaft

To evaluate the friction force along needle shaft ($F_f$), we adopt the method by Roesthuis *et al.*, [7]. The needle inside the tissue is divided into *n* unit. Each unit considered as rigid straight shaft, on which friction force $f$ is acted. Total friction force components in X- and Y-direction ($F_{fx}$ and $F_{fy}$) is obtained by integration over the insertion depth of needle (*p*):

$$F_{fx} = \int_{l-p}^{l} f \cos\theta(x) dx \tag{7}$$

$$F_{fy} = \int_{l-p}^{l} f \sin\theta(x) dx \tag{8}$$

## 3. Model of Needle-tissue Interaction

During insertion into a soft tissue, the needle can be considered as a cantilever beam supported by a series of spring, as shown in Figure 3. Taking into account the nonlinearity and imhomogeneity of soft tissue, we assume that this series of spring are nonlinear springs, each of which has stiffness ($K_s$) different from each other. The relationship between the force and deformation of nonlinear spring is expressed as:

$$F(x) = K_s (x + x^3) \tag{9}$$

When the needle is inserted into tissue, the cutting force on the needle tip is taken as input and cause the needle to deflect in transversal and axial direction. However, because

of high stiffness in axial direction, the axial deflection is negligible compared to transversal deflection.

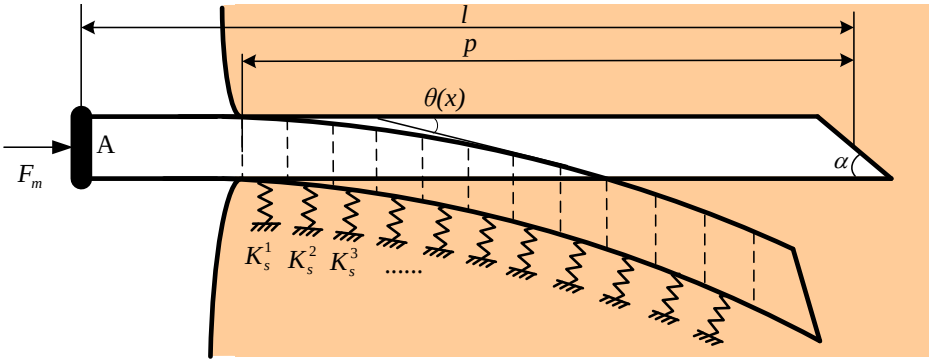


**Figure 3. Model of Needle-tissue Interaction**

The modeling of inserting a bevel-tipped needle into a soft tissue is discretized into a series of insertion steps, shown in Figure 4. In each step, the insertion depth ( $p$ ) is increased by $\Delta l$ and the additional deflection due to cutting force ( $F_c$ ) is calculated.

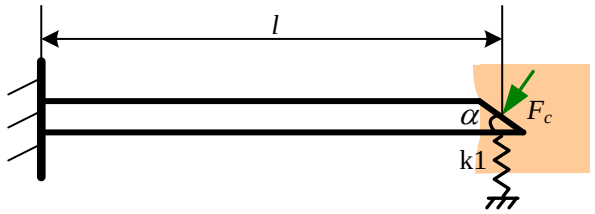


(a) Beginning of needle insertion

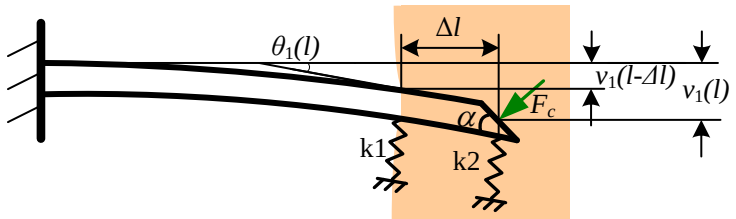


(b) Insertion step 1

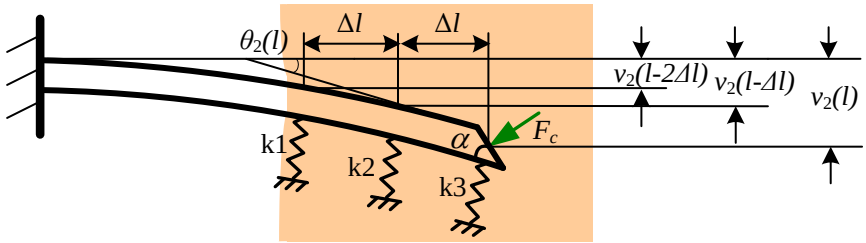


(c) Insertion step 2

**Figure 4. A Series of Insertion Steps of Needle Insertion into a Soft Tissue**

(1) Beginning of insertion

At the beginning of needle insertion, we assume the needle is supported by a spring $k1$ at needle tip and there is no deflection for needle (Figure 4 (a)).

(2) Insertion step 1

The insertion depth of needle is further increased with a distance $\Delta l$ (Figure 4 (b)); another spring $k2$ is added at the needle tip. The displacement function of needle is assumed as $v_1(x)$, the slope function of needle is $\theta_1(x)$.Thus, the deflection of the needle at the position of spring $k1$ is $v_1(l-\Delta l)$, and at spring $k2$ is $v_1(l)$. In this step, spring $k1$ is compressed with the deformation amount of $v_1(l-\Delta l)/\cos(\theta_1(l-\Delta l))$; while spring $k2$ is not compressed.

(3) Insertion step 2

Starting with step 1, the needle is further inserted with a distance $\Delta l$ and spring $k3$ is added at the needle tip (Figure 4(c)). The displacement function of needle is assumed as $v_2(x)$, the slope function of needle is $\theta_2(x)$. Thus, the deflection of needle at the position of spring $k1$ is $v_2(l-2\Delta l)$, spring $k2$ is $v_2(l-\Delta l)$, and spring $k3$ is $v_2(l)$. Spring $k1$ and $k2$ have the deformation amount of $v_2(l-2\Delta l)/\cos(\theta_2(l-2\Delta l))-v_1(l-\Delta l)/\cos(\theta_1(l-\Delta l))$ and $v_2(l-\Delta l)/\cos(\theta_2(l-\Delta l))-v_1(l)/\cos(\theta_1(l))$ respectively. Spring $k3$ is not compressed.

Following steps are similar, until the final insertion depth is reached.

## 4. Methods

Upon the model of needle-tissue interaction, Rayleigh-Ritz method based on principle of minimum potential energy is used to predict the deflection.

### 4.1. Rayleigh-Ritz Method

As mentioned above, the needle is considered as a cantilever beam supported by a series of nonlinear spring; and the process of needle insertion is discretized into a series of insertion steps. The deflected needle shape at any step of insertion $i$ is evaluated by minimizing the potential of the system. The system potential at step $i$ is given as

$$\Pi_i = (U_{Bi} + U_{Si}) - W_i \tag{10}$$

where, $U_{Bi}$ is the energy associated with needle bending; $U_{Si}$ denotes the elastic potential energy stored in the springs. While $W_i$ represents the work done by cutting force ($F_c$).

#### 4.1.1. Bending Energy

$U_{Bi}$ is the strain energy associated with transversal needle bending. At a certain step of insertion ($i$), the strain energy can be calculated with the beam theory as follows:

$$U_{Bi} = \frac{E_n I}{2}\int_0^l \left(\frac{d^2 v_i(x)}{dx^2}\right)^2 dx \tag{11}$$

Where, $E_n$ is the Young's modulus of the needle, and $I$ is the needle's second moment of inertia. $l$ is the length of the needle; $v_i(x)$ is the displacement function of needle at the step of insertion ($i$).

#### 4.1.2. Elastic Potential Energy in Springs

The elastic potential energy stored in a specified spring can be calculated by the difference in deflection between the current and previous needle deflection, thus the total energy is defined as the sum of the energies of all the individual springs.

$$U_{Si} = \sum_{k=1}^{i} \left\{ \begin{array}{l} \frac{1}{2} K_s^i \left[ \frac{v_i(l - k\Delta l)}{\cos(\theta_i(l - k\Delta l))} - \frac{v_{i-1}(l - (k-1)\Delta l}{\cos(\theta_{i-1}(l - (k-1)\Delta l)} \right]^2 \\ + \frac{1}{4} K_s^i \left[ \frac{v_i(l - k\Delta l)}{\cos(\theta_i(l - k\Delta l))} - \frac{v_{i-1}(l - (k-1)\Delta l}{\cos(\theta_{i-1}(l - (k-1)\Delta l)} \right]^4 \end{array} \right\} \tag{12}$$

To simplify the calculations, it is assumed that

$$\cos(\theta_i(l - k\Delta l)) = \cos(\theta_{i-1}(l - (k-1)\Delta l) \tag{13}$$

Therefore

$$U_{Si} = \sum_{k=1}^{i} \left\{ \frac{1}{2} K_s^i \left[ \frac{v_i(l - k\Delta l) - v_{i-1}(l - (k-1)\Delta l}{\cos(\theta_{i-1}(l - (k-1)\Delta l)} \right]^2 + \frac{1}{4} K_s^i \left[ \frac{v_i(l - k\Delta l) - v_{i-1}(l - (k-1)\Delta l}{\cos(\theta_{i-1}(l - (k-1)\Delta l)} \right]^4 \right\} \tag{14}$$

### 4.1.3. Work done by Cutting Force

The word done by cutting force $F_c$ is determined by the difference in tip deflection between adjacent two step of $i$ and $i-1$:

$$W_i = F_c^{i-1} \left[ \frac{v_i(l)}{\cos(\alpha + \theta_i(l))} - \frac{v_{i-1}(l)}{\cos(\alpha + \theta_{i-1}(l))} \right] \tag{15}$$

Due to the changes in the slope of needle tip is small relative to the bevel angle, in order to simplify the calculation, we assume that

$$\cos(\alpha + \theta_i(l)) = \cos(\alpha + \theta_{i-1}(l)) \tag{16}$$

According to equation (5), the cutting force at step of insertion $(i-1)$ is

$$F_c^{i-1} = F_{cx}^{i-1} / \sin(\alpha + \theta_{i-1}(l)) \tag{17}$$

So, the work done by cutting force at step of insertion $(i)$ is

$$W_i = \frac{2F_{cx}^{i-1}\left[v_i(l) - v_{i-1}(l)\right]}{\sin\left[2(\alpha + \theta_{i-1}(l))\right]} \tag{18}$$

## 4.2. Realization of Rayleigh-Ritz Method

In this section, the realization of Rayleigh-Ritz method is presented which is used to predict the amount of needle deflection.

### 4.2.1. Displacement Function of Needle

In order to obtain the needle deflection using Rayleigh-Ritz method, an assumed displacement function has to be defined which satisfies the geometric boundary conditions of the system. According to the knowledge of material mechanics, we select a third-order polynomial as the displacement function of needle, which is

$$v_i(x) = a_{i0} + a_{i1}x + a_{i2}x^2 + a_{i3}x^3 \qquad (0 \le x \le l) \tag{19}$$

The slope function of the needle is calculated by

 

$$\theta_i(x) = \arctan\left(\frac{dv_i(x)}{dx}\right) \approx \frac{dv_i(x)}{dx} \tag{20}$$

The displacement function $v_i(x)$ must satisfy the following geometric boundary conditions.

$$v_i(0) = 0 \tag{21}$$

$$\theta_i(0) = \frac{dv_i(x)}{dx}|_{x=0} = 0 \tag{22}$$

And then, applying the following stationary value condition of potential energy

$$\frac{\partial \Pi}{\partial a_{i2}} = \frac{\partial \Pi}{\partial a_{i3}} = 0 \tag{23}$$

The coefficients $a_{ik}$ ($k = 0,1,2,3$) of displacement function $v_i(x)$ can be calculated by solving equations (21) to (23).

#### 4.2.2. Solving of Cutting Force

According to formula (18), the horizontal tip force $F_{cx}$ is required in order to estimate needle deflection. To solve this, the process of needle insertion is regarded as quasi-static process. And at a given instant in time during insertion, the forces along the X-direction can be expressed as

$$F_m^i - F_{cx}^i - F_{fx}^i = 0 \tag{24}$$

Obviously, the cutting force $F_{cx}^i$ can be calculated by subtracting the friction force $F_{fx}^i$ from the insertion force $F_m^i$ if the value of friction force is known. The amount of friction force can be measured through experiment. We can use a robot to insert a needle with symmetrical tip into a soft tissue, and then the needle exits from the tissue by the same velocity of insertion. Since there is no cutting force and no bending during needle exit from tissue, the exiting force, which can be recorded by a force sensor mounted on the base of needle, is taken as the friction force.

#### 4.2.3. Determination of Spring Stiffness

According to the analysis in sub Section 2.1, the component in X-direction of cutting force on needle tip at the step of insertion $i$ can be calculated by

$$F_{cx}^i = \frac{K_t^i d^2}{\sin 2\alpha} \sin\left(\alpha + \theta_i(l)\right) \tag{25}$$

So the interaction stiffness of the needle-tissue per unit length $K_t^i$ (N/mm$^2$) can be derived as

$$K_t^i = \frac{F_{cx}^i \sin 2\alpha}{d^2 \sin\left(\alpha + \theta_i(l)\right)} \tag{26}$$

The stiffness of each spring is calculated by

$$K_s^i = K_t^i \cdot \Delta l \tag{27}$$

## 5. Experiments and Results

Needle insertion experiments are performed using a stainless steel needle with a bevel angle of 23°, diameter of 1.65mm, length of 170mm and Young's modulus of 200 Gpa. Agar is used as a phantom of soft tissue. The needle is inserted at the velocity of 5 mm/s.

Figure 5 shows the curves of insertion force and friction force versus insertion depth. Since the friction force is measured through exiting straightly from tissue, the friction force per unit needle length $f_f$ is equal to the slope of the friction force curve in Figure 5. It should be noted that, at the beginning of needle exit, the error of friction will increase because of the vibration of motor, shown as the friction force relative to insertion depth of 85 to 90mm, which is ignored. The calculated value e of $f_f$ is 0.01206 N/mm.

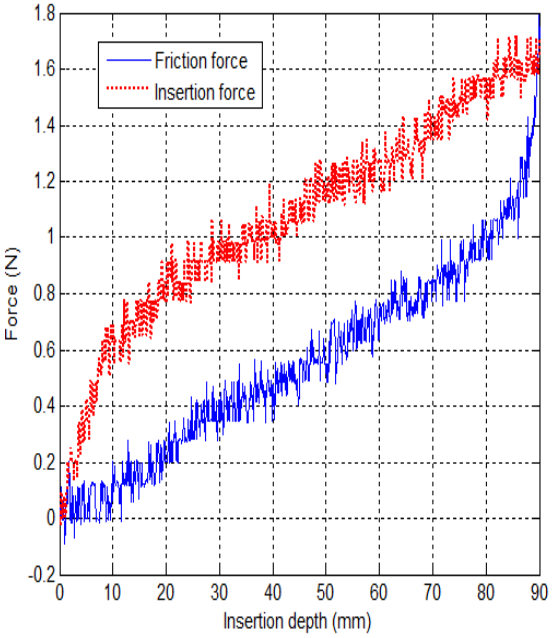


**Figure 5. Insertion Force and Friction Force VS Insertion Depth of Needle**

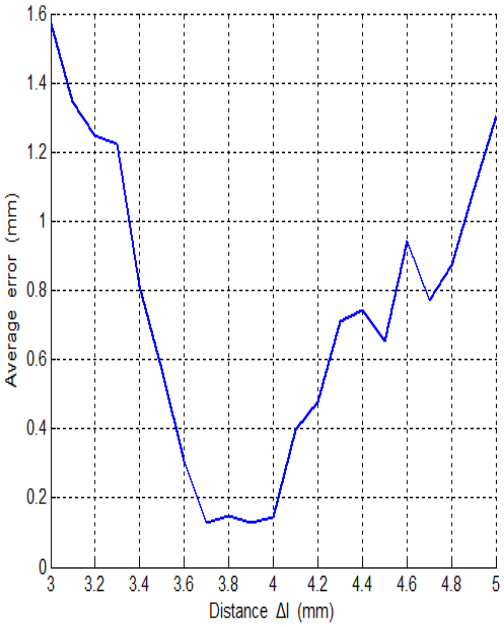


**Figure 6. Average Error between Simulated and Experimental Deflection VS Distance $\Delta l$**

The optimal value for the spring stiffness $K_s^i$ (also means the optimal value for distance ($\Delta l$) is found by minimizing the average of absolute error ($e_{ss}$) between simulated and experimental deflection of needle tip.

$$e_{ss} = \frac{1}{n}\sum_{i=1}^{n}\left|v_{sim}^{i}(l) - v_{\exp}^{i}(l)\right| \tag{28}$$

It can be seen from Figure 6 that the optimal value for distance $\Delta l$ is 3.9mm; the corresponding average error is 0.1281mm，and the corresponding stiffness of spring is shown in Figure 7. Obviously it is not constant.

In Figure 8, the simulated deflection is compared with the experimental deflection with $\Delta l$ =3.9. The maximum error is only 0.2549.

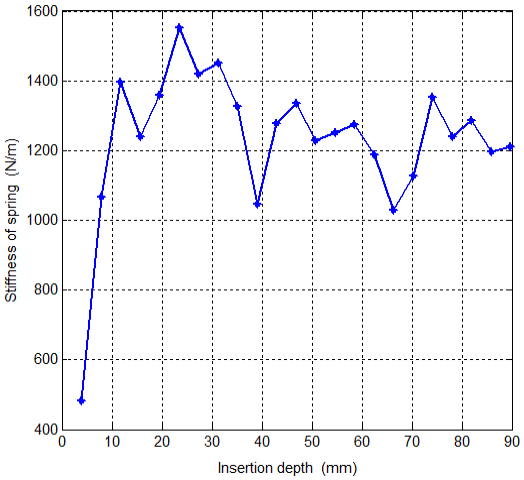


**Figure 7. The Stiffness of Springs Corresponding with $\Delta l$ =3.9**

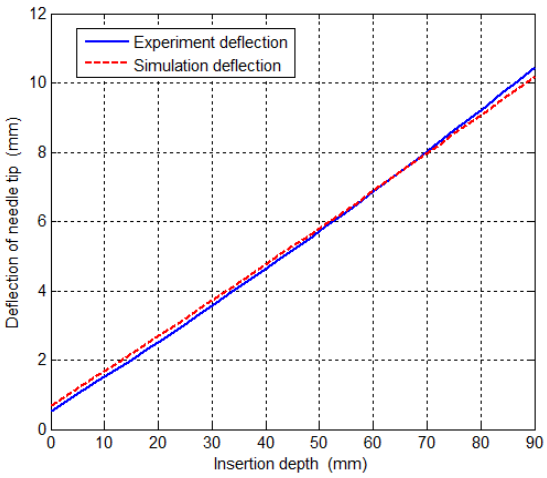


**Figure 8. Comparsion of Simulated and Experimental Deflection with $\Delta l$ =3**

## 6. Conclusions

(1) Needle-tissue interaction was modeled as a cantilever beam supported by a series of nonlinear springs each of which has stiffness different from each other. The stiffness was calculated through modeling the cutting force on the needle tip. The cutting force was extracted by subtracting the friction force from the insertion force.

(2) Based on the model of cantilever beam supported by a series of nonlinear springs, Rayleigh-Ritz method was used to predict the amount of needle deflection. Simulated needle deflection was compared to experimental needle deflection. It is found that the average error between simulated and experimental needle deflection is minimum when $\Delta l$ is 3.9 mm, correspondingly, the maximum of absolute error is only 0.2549 mm. The results indicate that nonlinear spring and variable stiffness are more consistent with the nonlinearity and imhomogeneity of soft tissue.

## Acknowledgements

This research was supported by the National Natural Science Foundation of China (Grant No. 51305107), the National Natural Science Foundation of Heilongjiang Province (Grant No. E201448), and the Heilongjiang Province Education Bureau Project (Grant No. 12531122).

## References

[1] N. Abolhassani1, R. Patel1 and F. Ayazi, "Needle control along desired tracks in robotic prostate brachytherapy", Proceedings of the IEEE International Conference on Systems, Man and Cybernetics, **(2007)**, pp. 3361-3366.

[2] D. Glozman and M. Shoham, "Image-guided robotic flexible needle steering", IEEE Transactions on Robotics, vol. 23, no. 3, **(2007)**, pp. 459-467.

[3] N. Abolhassani, R. V. Patel and F. Ayazi, "Minimization of needle deflection in robot-assisted percutaneous therapy", The International Journal of Medical Robotics and Computer Assisted Surgery, **(2007)**, pp. 140-148.

[4] A. Asadian, M. Kermani and R. Patel, "An analytical model for deflection of flexible needles during needle insertion", International Conference on Intelligent Robots and Systems (IROS), **(2011)**, pp. 2551-2556

[5] N. Abolhassani and R. V. Patel, "Deflection of a flexible needle during insertion into soft tissue", Proceedings of the 28th IEEE EMBS Annual International Conference, **(2006)**, pp. 3858–3861.

[6] N. Abolhassani1, R. Patel1 and F. Ayazi, "Effects of Different Insertion Methods on Reducing Needle Deflection", Proceedings of the 29th Annual International Conference of the IEEE EMBS, **(2007)**, pp. 491-494.

[7] Roy J. Roesthuis, Youri R. J. van Veen, A. Jahya and S. Misra, "Mechanics of Needle-Tissue Interaction", IEEE/RSJ International Conference on Intelligent Robots and Systems, **(2011)**, pp. 2557-2563.
[8] R. J. Roesthuis, M. Abayazid and S. Misra, "Mechanics-based model for predicting in-plane needle deflection with multiple bends", Proceedings of the IEEE RAS/EMBS Int. Conf. on Biomedical Robotics and Biomechatronics, **(2012)**, pp. 69- 74.
[9] J. J. Wang, X. P. Li, J. J. Zheng and D. Sun, "Mechanics-Based Modeling of Needle Insertion into Soft Tissue", IEEE/ASME International Conference on Advanced Intelligent Mechatronics (AIM), **(2013)**, pp. 38-43.
[10] H. Sadjadi, K. Hashtrudi-Zaad and G. Fichtinger, "Needle Deflection Estimation using Fusion of Electromagnetic Trackers", 34th Annual International Conference of the IEEE EMBS , **(2012)**, pp. 952-955.
[11] A. M. Okamura, C. Simone and M. D. O'Leary, "Force modeling for needle insertion into soft tissue", IEEE Transactions on Biomedical Engineering, vol. 51, no. 10, **(2004)**, pp. 1707–1716.
[12] S. Misra, K. B. Reed, K. T. Ramesh and A. M. Okamura, "Observations of needle-tissue interactions", 31st Annual International Conference of Engineering in Medicine and Biology Society (EMBS), **(2009)**, pp. 262–265.

 